Cross section measurements of the $^{14}N(^{3}He,p)^{16}O$ and $^{14}N(^{3}He,\alpha)^{13}N$ reactions between 1.6 and 2.8 MeV

Terwagne, Guy; Cohen, David D.; Collins, George A.

Published in:
Nuclear Instruments and Methods in Physics Research, Section B: Beam Interactions with Materials and Atoms

DOI:
10.1016/0168-583X(94)95335-X

Publication date:
1994

Document Version
Early version, also known as pre-print

Nuclear Instruments and Methods in Physics Research B 84 (1994) 415–420
North-Holland

NIM B
Beam Interactions with Materials & Atoms

Cross-section measurements of the $^{14}N(^{3}He,p)^{16}O$ and $^{14}N(^{3}He,\alpha)^{13}N$ reactions between 1.6 and 2.8 MeV

G. Terwagne [a,*], D.D. Cohen [b] and G.A. Collins [b]

[a] *Laboratoire d'Analyses par Reactions Nucleaires, rue Muzet 22, B5000 Namur, Belgium*
[b] *Lucas Heights Research Laboratories, Australian Nuclear Science and Technology Organisation, Private Mail Bag 1, Menai NSW 2234, Australia*

Received 25 June 1993 and in revised form 8 November 1993

The cross-sections of the $^{14}N(^{3}He,p_i)^{16}O$ ($i = 1,2,3,4,5,7$) and $^{14}N(^{3}He,\alpha_0)^{13}N$ reactions have been measured for ^{3}He incident energies between 1.6 and 2.8 MeV. These reactions offer an alternative to the $^{14}N(d,p)^{15}N$ and $^{14}N(d,\alpha)^{12}C$ nuclear reactions for profiling of nitrogen in the first few microns below the surface. The technique has been applied to tool steels treated by Plasma Immersion Ion Implantation, where treatment at elevated temperatures leads to diffusion of the nitrogen to depths well beyond the implantation range. Simultaneous measurement of the carbon profile can be made using the $^{12}C(^{3}He,p)^{14}N$ reactions.

1. Introduction

Light elements such as carbon, nitrogen and oxygen play an important role in the surface treatment of steels by techniques such as ion implantation, thermochemical diffusion (nitriding, carburising), Chemical Vapour Deposition (CVD) and Physical Vapour Deposition (PVD). Depth profiling of these light elements is usually performed by means of resonant nuclear reaction analysis (RNRA) induced by protons or alpha particles. RNRA gives a good depth resolution but only for one element at a time [1]. Non-resonant nuclear reaction analysis (NRA), induced by deuterons or ^{3}He particles, can be used for profiling more than one light element [2]. The cross-sections for the deuteron reactions are large but the neutrons produced by these reactions prevent their widespread application. An alternative is to use ^{3}He as the incident particle and induce $(^{3}He,p)$ or $(^{3}He,\alpha)$ reactions on the light elements. These reactions produce less neutrons and are more sensitive near the surface since the stopping power is higher for ^{3}He than for deuterons of the same energy. Although the Q-values for the $(^{3}He,p)$ or $(^{3}He,\alpha)$ reactions on light elements are high, the cross-sections are smaller than the reactions induced by deuterons. For example, the cross-section of the $^{14}N(d,\alpha_0)^{12}C$ reaction is four times higher than the cross-section of the $^{14}N(^{3}He,\alpha_0)^{13}N$ reaction in the same geometry and in the same range of incident particle energies [3,4].

Data for the $^{14}N(^{3}He,\alpha)^{13}N$ and the $^{14}N(^{3}He,p)^{16}O$ reactions are not available in the literature for incident particle energies below 2.5 MeV because the cross-sections are very small [4–7] although the high Q-values for these reactions (Table 1) makes them very suitable for the depth profiling of nitrogen. In this paper, we measured the cross-sections for the $^{14}N(^{3}He,\alpha_0)^{13}N$ and the $^{14}N(^{3}He,p_i)^{16}O$ ($i = 1,2,3,4,5,7$) reactions for an incident energy varying between 1.6 and 2.8 MeV and reactions angle of 90° and 135°. We have used these reactions to measure the nitrogen depth profile in tool steel treated by Plasma Immersion Ion Implantation [8] at various temperatures.

2. Experimental procedure

To provide an absolute measurement of the cross-sections, a set of standards was prepared by conventionally implanting silicon wafers with 50 keV $^{14}N^{+}$ ions at a dose of 5.6×10^{17} ions/cm^2 using the implantation facilities of the National Measurement Laboratory (Sydney, Australia). The operating pressure was 2.5×10^{-6} mbar and the specimens were implanted at 7° relative to the normal to avoid channelling of the implanted species. A retained dose of 3.1×10^{17} N/cm^2 was measured with the resonant nuclear reaction $^{14}N(\alpha,\gamma)^{18}F$ at 1531 keV using the 2.5

* Corresponding author, tel. +32 81 731267, fax +32 81 737938, e-mail larn@bnandp51.

SSDI 0168-583X(93)E0862-B

Table 1
Q-values and calculated energies of particles emitted at 90° and 135° for the $^{14}N(^3He,p_i)^{16}O$ (for $i = 0,1,\ldots,9$), $^{14}N(^3He,\alpha_0)^{13}N$, $^{14}N(^3He,d_0)^{15}O$ and $^{12}C(^3He,p_i)^{14}N$ (for $i = 1,2,3$) reactions. The energy of the incident particle is 2.7 MeV and the energies of the emitted particles are calculated before the mylar absorber

Reaction	Q-value (MeV)	E_p (90°) (MeV)	E_p (135°) (MeV)
$^{14}N(^3He,p_0)^{16}O$	15.243	16.401	15.465
$^{14}N(^3He,p_1)^{16}O$	9.194	10.711	9.959
$^{14}N(^3He,p_2)^{16}O$	9.113	10.634	9.885
$^{14}N(^3He,p_3)^{16}O$	8.324	9.892	9.171
$^{14}N(^3He,p_4)^{16}O$	8.126	9.706	8.992
$^{14}N(^3He,p_5)^{16}O$	6.371	8.055	7.407
$^{14}N(^3He,p_7)^{16}O$	5.396	7.138	6.529
$^{14}N(^3He,p_8)^{16}O$	4.890	6.662	6.075
$^{14}N(^3He,p_9)^{16}O$	4.291	6.098	5.538
$^{14}N(^3He,\alpha_0)^{13}N$	10.024	9.251	7.916
$^{14}N(^3He,\alpha_1)^{13}N$	7.659	7.443	6.256
$^{14}N(^3He,\alpha_2)^{13}N$	6.513	6.567	5.458
$^{14}N(^3He,\alpha_3)^{13}N$	6.477	6.539	5.433
$^{14}N(^3He,d_0)^{15}O$	1.803	3.492	2.917
$^{12}C(^3He,p_0)^{14}N$	4.779	6.435	5.786
$^{12}C(^3He,p_1)^{14}N$	2.466	4.277	3.754
$^{12}C(^3He,p_2)^{14}N$	0.832	2.752	2.339

MV Van de Graaff accelerator of the LARN (Namur, Belgium). This nitrogen profiling technique has been described in previous papers [1]. The standards made by ion implantation consisted of a thin layer (100 nm) of stable silicon nitride [9]. The implanted area was about 7 cm^2 and the homogeneity of the implanted dose was verified by NRA.

Samples of a high alloy proprietary steel marketed as Viking (0.5% C, 1.0% Si, 0.5% Mn, 8.0% Cr, 1.5% Mo and 0.5% V (weight percent)) were tempered at 540°C and treated by Plasma Immersion Ion Implantation (PI^3) at 300°C and 400°C in the PI^3 facility at Lucas Heights with a nominal nitrogen dose of 1×10^{18} atoms/cm^2. This involved immersion of the samples in a nitrogen plasma of density 1×10^{10}/cm^3 for 2 hours at the treatment temperature.

The cross-sections of the reactions $^{14}N(^3He,p_i)^{16}O$ (for $i = 1,2,3,4,5,7$) and $^{14}N(^3He,\alpha_0)^{13}N$ were measured on the silicon standards between 1.6 and 2.8 MeV using the 3 MV Van der Graaff accelerator at Lucas Heights. A 50 mm^2 silicon surface barrier detector of 1 mm thickness was placed at 5.8 cm from the beam spot on the sample. A slit of 2 mm width and 8 mm height was placed in front of the detector in order to define the reaction angle. A mylar absorber foil of 12 μm was placed in front of the detector in order to stop the scattered ^3He particles. The cross-sections were measured at two different angles: 90° and 135°. The solid angle of the detector was measured by conventional RBS with 2.0 MeV alpha particles on a calibrated sample of Bi implanted Si wafer. This standard was prepared at Harwell (UK) with a dose of 4.77×10^{17} atoms/cm^2 [10]. The measured solid angle was 4.687 msr. The sample and the standards were tilted at 50° relative to the normal of the surface in order to avoid channelling during measurements and to improve the depth resolution.

Typical beam currents of 400 nA were used during the NRA measurements on an area of about 10 mm^2, while a few nA was sufficient for the RBS measurements. The stability of the silicon nitride layer was verified at this current density. The total integrated charge for the NRA measurements was either 500 or 1000 μC, depending on the statistics required.

The energy of the Van der Graaff accelerator was measured precisely by calibrating the magnetic field prior to measuring the cross-sections. The neutron threshold of the $^{12}C(^3He,n)^{14}O$ reaction which occurs at $E_{th} = 1.435$ MeV and the $^7Li(p,n)^7Be$ reaction at $E_{th} = 1880.6$ keV were used. The known $^{27}Al(p,\gamma)^{28}Si$ resonance at $E_R = 991.8$ keV and the $^{16}O(^3He,\alpha_0)^{15}O$ resonant reaction at $E_R = 2.380$ MeV [11] on a thin Ta_2O_5 target were also measured in order to calibrate the magnetic field over a wide range of current.

The samples treated by the PI^3 process were measured in the same geometry as the standards with a total integrated charge of 500 μC. The time required to record a typical spectrum of a treated tool steel was about 20 minutes.

3. Cross-section measurements

A typical spectrum measured at 90° with 2.7 MeV ^3He particles on the ^{14}N implanted Si standard is shown in Fig. 1. The $p_{1,2}$ to p_7 peaks and the α_0 peaks are well isolated and the background under these peaks is almost zero. The energy of the emitted particles for reaction angles of 90° and 135° is shown along with the Q values in Table 1. The energy of the p_1 and the p_2 components are too close together to separate and can be consider as a single group. The α_2 and α_3 components are also very close in energy. At a reaction angle of 90°, the peaks p_8 and α_1 interfere once energy loss in the absorber foil is considered. The peaks associated with the $^{14}N(^3He,p_i)^{16}O$ reactions (for $i > 9$) are too close together to obtain reliable measurements. For these reasons we have only measured the cross-sections for the isolated peaks, that is $p_{1,2}$ to p_7 and α_0. The p_0 protons group has not been measured because the energy of those protons should be degrated in an absorber foil so thick that the results will not be available for depth profiling. The huge peak around 3.2 MeV is attributed to the $^{14}N(^3He,d_0)^{15}O$ reaction

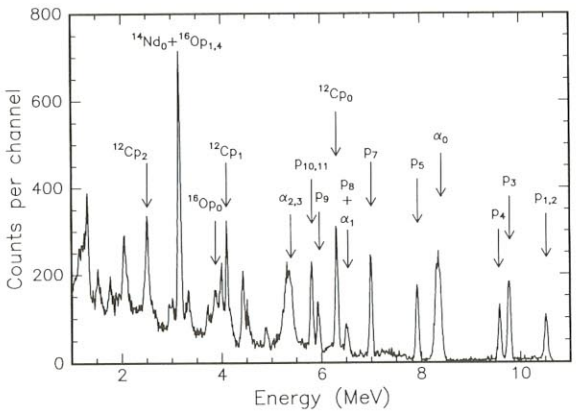

Fig. 1. Typical spectrum measured at a reaction angle of 90° with 2.7 MeV ^{3}He particles on the silicon wafer standard. The integrated charge was 500 μC and the incident angle was 50°. The p_i (for $i = 1,2,\ldots,11$) and α_i (for $i = 0,1,2,3$) labels are attributed respectively to the $^{14}N(^3He,p_i)^{16}O$ and the $^{14}N(^3He,\alpha_i)^{13}N$ reactions, while the other labels are attributed directly to the ^{3}He reaction on the indicated element.

but it also interferes with the p_{1-4} peaks from the $^{16}O(^3He,p)^{18}F$ reactions.

In Fig. 1, the p_0 to p_2 peaks associated with the $^{12}C(^3He,p_i)^{14}N$ reactions are due to surface contamination of the standard. Since the cross-sections of $^{12}C(^3He,p_i)^{14}N$ are much higher than the cross-sections on nitrogen [12] these peaks appear in the spectrum although the actual amount of carbon on the surface is small. The p_0 peak of carbon is isolated in between p_8 and p_9 peaks of nitrogen and can be used for analysing carbon together with nitrogen. Unfortunately, the cross-sections of the $^{12}C(^3He,p_i)^{14}N$ reactions are only known below 2.4 MeV at a reaction angle of 90° [12].

The cross-sections were obtained from the following formula:

$$d\sigma/d\Omega = \Delta A \cos(90-\alpha)/\Delta\Omega N_M N_1,$$

where ΔA is the area under each peak, $\Delta\Omega$ is the solid angle of the detector, α is the incident angle, N_M is the number of nitrogen atoms (atoms/cm^2), and N_1 is the number of incident particles.

Fig. 2 shows the measured cross-section for $^{14}N(^3He,p_i)^{16}O$ (for $i = 1,2,3,4,5,7$) and $^{14}N(^3He,\alpha_0)^{13}N$ reactions at a reaction angle of 90°. The curves have been drawn as a guide. The absolute error was estimated to be 10% and arises from the precision of the estimation of the solid angle, the integration of the incident current, the measurement of the retained dose in the implanted standard and the statistical error from measuring the area of each peak. Our data is in good agreement with the data obtained by Knudson and Young [4] for the $^{14}N(^3He,\alpha_0)^{13}N$ over the energy range where the measurements overlap. For comparison, the data of Knudson and Young is shown in Fig. 2f by the unfilled triangles. For the $^{14}N(^3He,p_i)^{16}O$ reactions, only data for the p_0 reaction is available in the literature over the range of energies that we have used [5] but unfortunately our detector was not thick enough to detect the p_0 proton group.

All measured cross-sections increase monotonically with incident energy and no resonance peaks have been found. The values of the cross-sections obtained at a reaction angle of 90° are tabulated in Table 2.

Fig. 3 shows the measured cross-section for $^{14}N(^3He,p_i)^{16}O$ ($i = 1,2,3,4,5,7$) and $^{14}N(^3He,\alpha_0)^{13}N$ reactions at a reaction angle of 135°. As in Fig. 2, the solid line has been as a guide and the absolute error is approximately 10%. There is no data in the literature to which we can compare our measurements. Most of the cross-sections at this angle also monotonically in-

Table 2
Tabulation of the differential cross sections (mb/sr) for the $^{14}N(^3He,p_i)^{16}O$ (for $i = 1,2,3,4,5,7$) and the $^{14}N(^3He,\alpha_0)^{13}N$ reactions at a reaction angle of 90°

Energy (MeV)	$\sigma(p_{1,2})$ (mb/sr)	$\sigma(p_3)$ (mb/sr)	$\sigma(p_4)$ (mb/sr)	$\sigma(p_5)$ (mb/sr)	$\sigma(p_7)$ (mb/sr)	$\sigma(\alpha a_0)$ (mb/sr)
1.589	0.013	0.007	0.008	0.011	0.008	0.016
1.787	0.022	0.014	0.016	0.021	0.015	0.030
1.984	0.041	0.027	0.027	0.033	0.025	0.050
2.083	0.049	0.034	0.036	0.039	0.037	0.063
2.182	0.061	0.047	0.045	0.046	0.038	0.082
2.231	0.070	0.053	0.047	0.052	0.045	0.089
2.281	0.073	0.057	0.046	0.056	0.054	0.11
2.358	0.090	0.074	0.058	0.070	0.067	0.135
2.478	0.102	0.099	0.070	0.089	0.094	0.21
2.577	0.112	0.125	0.079	0.100	0.112	0.27
2.676	0.123	0.145	0.091	0.138	0.146	0.33
2.775	0.122	0.158	0.098	0.109	0.176	0.38

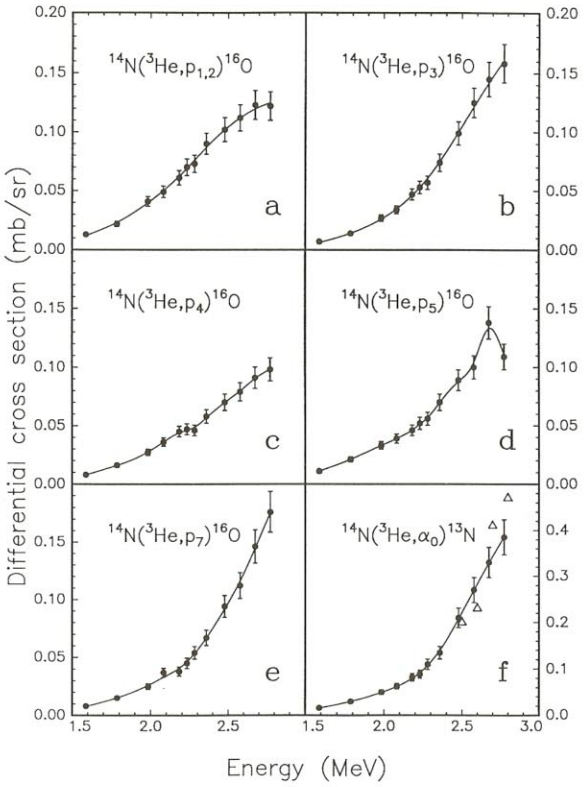

Fig. 2. Differential cross sections for the $^{14}N(^3He,p_i)^{16}O$ (for $i = 1,2,3,4,5,7$) and the $^{14}N(^3He,\alpha_0)^{13}N$ reactions at a reaction angle of 90°. The full curves have been drawn as a guide. The open triangles in (f) represent the data of Knudson and Young [4].

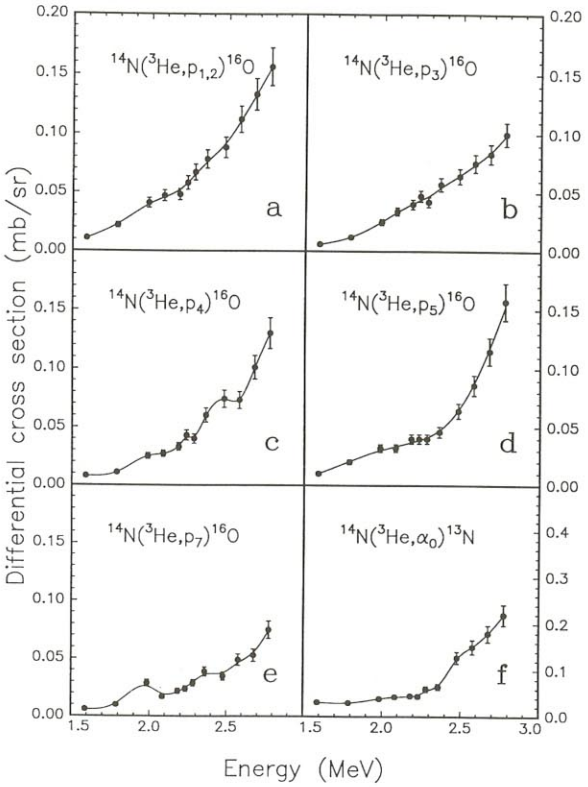

Fig. 3. Differential cross-sections for the $^{14}N(^3He,p_i)^{16}O$ (for $i = 1,2,3,4,5,7$) and the $^{14}N(^3He,\alpha_0)^{13}N$ reactions at a reaction angle of 135°. The full curves have been drawn as a guide.

crease with incident energy although the p_4 and p_7 cross-sections show some variation. We have tabulated the measured cross-section values at a reaction angle of 135° in Table 3. At low energy (1.589 MeV), there is an interference between the p_5 and the α_0 peaks. Two Gaussians have been fitted to the experimental data to obtain the area of both peaks. The widths of the Gaussians were set to the same value as the peaks obtained at 1.787 MeV and the position and areas

Table 3
Tabulation of the differential cross sections (mb/sr) for the $^{14}N(^3He,p_i)^{16}O$ (for $i = 1,2,3,4,5,7$) and the $^{14}N(^3He,\alpha_0)^{13}N$ reactions at a reaction angle of 135°

Energy (MeV)	$\sigma(p_{1,2})$ (mb/sr)	$\sigma(p_3)$ (mb/sr)	$\sigma(p_4)$ (mb/sr)	$\sigma(p_5)$ (mb/sr)	$\sigma(p_7)$ (mb/sr)	$\sigma(\alpha_0)$ (mb/sr)
1.589	0.011	0.006	0.008	0.010	0.006	0.031
1.787	0.022	0.012	0.011	0.020	0.010	0.030
1.984	0.041	0.025	0.025	0.032	0.029	0.039
2.083	0.047	0.034	0.027	0.032	0.017	0.043
2.182	0.048	0.040	0.033	0.040	0.022	0.045
2.231	0.058	0.047	0.043	0.040	0.024	0.044
2.281	0.067	0.042	0.040	0.040	0.029	0.060
2.358	0.078	0.057	0.060	0.046	0.039	0.065
2.478	0.088	0.064	0.074	0.064	0.035	0.13
2.577	0.112	0.075	0.073	0.086	0.049	0.15
2.676	0.133	0.083	0.101	0.115	0.053	0.18
2.775	0.156	0.100	0.130	0.157	0.075	0.22

were set as free parameters in a χ^2-minimisation algorithm [13].

In general, the measured cross-sections are lower at a reaction angle of 135° than at 90°. This is consistent with previous measurements of these cross-sections at higher incident energies [4–6].

4. Application to PI^3 treated tool steel

The cross-sections obtained in this work were used for measuring the nitrogen depth profile of PI^3 treated Viking tool steel. At the treatment temperatures of 300°C and 400°C nitrogen can diffuse over a range of several microns [14]. The treated samples were analysed with 2.7 MeV ^{3}He particles impinging on the surface of the steel with an angle of 50° relative to the normal. The spectrum recorded for the sample treated at 300°C is shown in Fig. 4a. The range of 2.7 MeV ^{3}He particles in steel is about 4.5 μm. In the inset of Fig. 4a, the depth scale for the $Np_{1,2}$ peak has been obtained from the stopping power and density of Viking tool steel. The nitrogen depth profile over a range of 2 μm can be obtained by correcting the experimental data with the cross-section data. It is also possible to improve the nitrogen profile further by removing the contribution of the p_3 and the p_4 peaks. These calculations have been made by using the SENRAS program [15] and the full curve in the inset of Fig. 4a shows the result of the simulation. The simulation assumes that there are two nitrogen-containing layers in the surface of this sample – one of 2000×10^{15} at./cm^2 thickness containing 23 at.% of nitrogen and a deeper one of $15\,000 \times 10^{15}$ at./cm^2 thickness containing around 13 at.% of nitrogen. The wide peaks around 6, 4 and 2 MeV are due respectively to $^{12}C(^3He,p_0)^{14}N$, $^{12}C(^3He,p_1)^{14}N$ and $^{12}C(^3He,p_2)^{14}N$ reactions and, in the absence of cross-section data, can be attributed in part to the 2.3 at.% of carbon normally in Viking tool steel. In Fig. 4b, we show the spectrum obtained for the same steel after PI^3 treatment at 400°C. The inset shows the simulated spectrum for the $Np_{1,2}$, Np_3 and Np_4 components. It is immediately obvious that nitrogen diffuses more deeply in the 400°C treated steel. We can observe in Fig. 4b that the carbon peaks Cp_0, Cp_1 and Cp_2 have a large component at the high energy side, implying that the concentration of carbon has increased near the surface. The simulation again involves two layers – the first of 1000×10^{15} at./cm^2 thickness containing 31 at.% of nitrogen and approximately 6 at.% of carbon and the second, deeper layer of $30\,000 \times 10^{15}$ at./cm^2 thickness containing approximately 20 at.% of nitrogen.

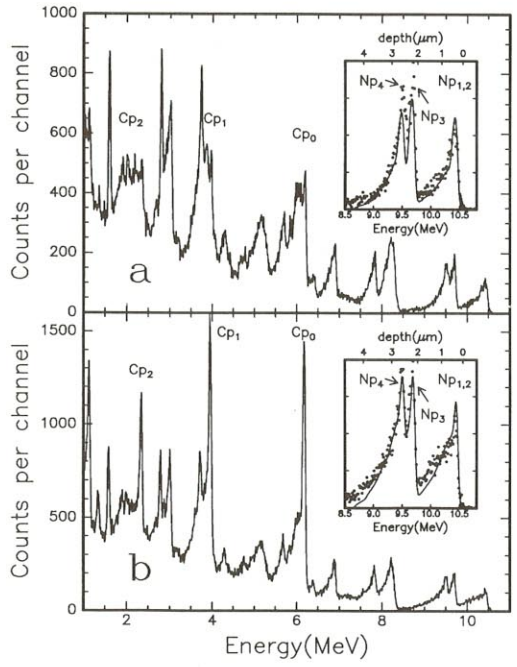

Fig. 4. Particle spectra of PI^3 treated Viking tool steel at various temperatures: (a) 300°C and (b) 400°C. For both spectra, the integrated charge was 500 μC, the incident angle was 50° and the reaction angle was 90°. The insets show an enlargement of the high energy protons, and the full curves in the insets have been obtain by simulations with the SENRAS code [15].

5. Conclusions

The cross-sections of the $^{14}N(^3He,p_i)^{16}O$ (for i = 1,2,3,4,5,7) and $^{14}N(^3He,\alpha_0)^{13}N$ reactions have been measured for ^{3}He incident energies between 1.6 and 2.8 MeV. Despite the small value of the cross-sections, these nuclear reactions are a powerful alternative to the $^{14}N(d,p)^{15}N$ or $^{14}N(d,\alpha)^{12}C$ reactions for measuring the nitrogen depth profiles. Due to the high Q-values of the reactions, a thick silicon surface barrier detector, able to detect 10 MeV protons, is required but the background under the nitrogen peaks is almost zero. At an incident energy of 2.7 MeV, the depth profile of nitrogen can be obtained from the $p_{1,2}$ peak over a range of 2 μm in a tool steel.

Carbon can be analysed simultaneously with nitrogen by measuring the p_0 peak but the cross-sections of the $^{12}C(^3He,p_i)^{14}N$ reactions have yet to be measured for energies greater than 2.4 MeV in our geometry of detection.

A thicker silicon surface barrier detector is necessary for measuring the protons of the $^{14}N(^3He,p_0)^{16}O$ reactions because their energy is about 16.5 MeV. From this reaction it should be possible to obtain a clear nitrogen depth profile over a few microns, with

the ultimate profiling depth depending only on the energy of the incident particle.

Acknowledgements

We wish to thank Dr. Mike Kenny of the CSIRO Division of Applied Physics for implanting the silicon standards. This work was performed whilst one of us (G.T.) was a visiting fellow at the Australian Nuclear Science and Technology Organisation.

References

[1] G. Terwagne, S. Lucas and F. Bodart, Nucl. Instr. and Meth. B 66 (1992) 262.
[2] C.R. Gosset, Nucl. Instr. and Meth. 218 (1983) 149.
[3] G. Debras and G. Deconninck, J. Radioanal. Chem. 38 (1977) 193.
[4] A.R. Knudson and F.C. Young, Nucl. Phys. A 149 (1970) 323.
[5] S. Gorodetzky, G. Bassompierre, C. St-Pierre, A. Gallmann and P. Wagner, Nucl. Phys. 43 (1963) 92.
[6] P. Guazzoni, S. Micheletti, M. Pignanelli, F. Gentilin and F. Pellegrini, Phys. Rev. C 4 (1971) 1086.
[7] O.M. Bilaniuk and W. Parker Alford, Bull. Am. Phys. Soc 7 (1962) 71.
[8] J. Tendys, I.J. Donnelly, M.J. Kenny and J.T.A. Pollock, Appl. Phys. Lett. 53 (1988) 2143.
[9] J.R. Bird and J.S. Williams, Ion Beams for Material Analysis (Academic Press, Sydney, Australia, 1989) p. 581.
[10] J.A. Davies, T.E. Jacman, H.L. Eschbach, W. Domba, U. Watjen and D. Chivers, Nucl. Instr. and Meth. B 15 (1986) 238.
[11] D.D. Cohen, G.M. Bailey and N. Dytlewski, Nucl. Instr. and Meth. B 64 (1992) 413.
[12] S.Y. Tong, W.N. Lennard, P.F.A. Alkemade and I.V. Mitchell, Nucl. Instr. and Meth. B 54 (1990) 91.
[13] P.R. Bevington, Data Reduction and Error Analysis for the Physical Sciences (McGraw-Hill, New York, San Francisco, London, 1968) p. 204.
[14] M. Samandi, A. Pauza, G. Hatziandoniou, H. Yasbandha, R. Hutchings, G.A. Collins and J. Tendys, Surf. Coat. Technol. 54/55 (1992) 447.
[15] G. Vizkelethy, Nucl. Instr and Meth. B 45 (1990) 1.